

Effects of Process Parameters in Synthesizing Sn Nanoparticles via Chemical Reduction

Sang-Soo Chee and Jong-Hyun Lee*

Department of Materials Science & Engineering, Seoul National University of Science and Technology,
Seoul 139-743, Korea

(received date: 17 August 2011 / accepted date: 22 November 2011)

In order to prepare solder particles for fine pitch interconnections, Sn nanoparticles were synthesized via chemical reduction methods. A number of the process parameters, i.e., injection rate of a precursor solution, application of sonication, reaction temperature, types of reaction medium and capping agent, and drying temperature, are varied in order to study their effect on this process. Using a methanol solution containing 1,10-phenanthroline monohydrate, the size of Sn nanoparticles collected after the synthesis decreases as the injection rate increases. An increase in the drying temperature strengthens the degree of agglomeration between Sn nanoparticles, and, in addition, the application of sonication accelerates the process of agglomeration and aggregation between nanoparticles during synthesis. Much smaller Sn nanoparticles are synthesized in diethylene-glycol solutions containing PVP, compared to the methanol solutions with 1,10-phenanthroline monohydrate. In the synthesis using diethylene-glycol solutions, the Sn nanoparticle size increases quickly with the reaction temperature.

Keywords: Sn nanoparticles, chemical reduction, injection rate, sonication, reaction temperature

1. INTRODUCTION

Solders are vital interconnection materials that enable the formation of both electrical and mechanical joints during the assembly of electronic products.^[1-3] Over the past few decades, the usage of Pb-free solders has stabilized technically; however, there is a consistent requirement for solder paste with the capability of being applied to finer pitch interconnections. To enhance the fine pitch capability of solder paste, nano-sized solder particles, which are included in the solder paste, must be adopted, instead of the present micro-sized particles.^[4,5]

Although physical processes, such as the spark erosion or arc discharge method, have been studied during recent years,^[6-8] the most promising process for fabricating solder nanoparticles is judged to be a chemical reduction method considering productivity and size uniformity.^[9-17] Nevertheless, research into the effects of process parameters in the synthesis of Sn nanoparticles via chemical reduction is surprisingly rare.

In this study, experiments focusing on the effects of process parameters, which include drying conditions as well as synthesis conditions, were conducted during the reducing

synthesis of Sn nanoparticles. The size and morphology of the synthesized Sn nanoparticles were analyzed with respect to the injection rate of a precursor, application of sonication, types of reaction medium and capping agent, and reaction temperature. In addition, the effect of the drying temperature was also investigated.

2. EXPERIMENTAL

In this study, tin(II) 2-ethylhexanoate ($[\text{CH}_3(\text{CH}_2)_3\text{CH}(\text{C}_2\text{H}_5)\text{CO}_2]_2\text{Sn}$) of ~95% (Sigma-Aldrich Chemical Co.) was used as a common precursor agent for synthesizing Sn nanoparticles. Methanol (99.9% purity, Duksan Pure Chemicals Co. Ltd.) and 1,10-phenanthroline monohydrate ($\text{C}_{12}\text{H}_8\text{N}_2 \cdot \text{H}_2\text{O}$) (Sigma-Aldrich Chemical Co.) were used as an initial reaction medium and capping agent, respectively. In further experiments, the methanol was exchanged with diethylene-glycol (DEG) (99% purity, Sigma-Aldrich Chemical Co.), and the 1,10-phenanthroline monohydrate with polyvinylpyrrolidone (PVP) ($M_w = 1300000$, Aldrich Chemical Co.). Sodium borohydride (NaBH_4) (99.99% purity, Aldrich Chemical Co.) was used as a reducing agent throughout.

In a typical synthesis, 0.3 g 1,10-phenanthroline monohydrate (or 1 g PVP) and 2 g sodium borohydride were dissolved completely in 100 ml methanol (or DEG) for 1 h.

*Corresponding author: pljh@snut.ac.kr
©KIM and Springer

The tin(II) 2-ethylhexanoate was injected into the methanol (or DEG) solution under stirring at room temperature, using a dispenser capable of different injection rates. After the immediate initiation of the reducing reaction, the solution was magnetically stirred for 1 h as a holding step in order to complete the reaction. In another batch, this holding step was performed in a sonication bath. The solution containing synthesized Sn nanoparticles was enriched at low centrifuge speeds of 4000 rpm (with methanol) and 6000 rpm (with DEG) to minimize agglomeration between nanoparticles. The enriched solutions were mainly dried at 60°C in a low-vacuum chamber to elevate the drying rate. For the sake of comparison, some samples were dried at room temperature or at approximately -70°C. When DEG was used as the reaction medium, it was repetitively exchanged with methanol during centrifuging, because drying at 60°C with DEG takes a considerable time owing to its low volatility. The size and morphology of the final Sn nanoparticles were observed using a field emission scanning electron microscope (FE-SEM).

3. RESULTS AND DISCUSSION

Figure 1 shows SEM images of the final Sn nanoparticles with respect to the rate at which the tin(II) 2-ethylhexanoate precursor was injected into the methanol solution containing 1,10-phenanthroline monohydrate and sodium borohydride at room temperature. At an injection rate of

1.5 ml/min, the particle size can be observed in the images (Fig. 1(a, b)) to be 40-400 nm in diameter (average diameter = 167.7 nm). In contrast, the size of the Sn nanoparticles formed after the injection rate is increased to 3 ml/min (Fig. 1(d, e)) was measured as 30-300 nm (average diameter = 123.6 nm), indicating a decrease in average size. This result implies that the size and size distribution of nanoparticles synthesized via chemical reduction is appreciably affected by the injection rate, i.e., the amount of Sn ions introduced to the medium per unit time. Park *et al.*^[18] reported that nanoparticles became smaller in size and narrower in size distribution as the injection rate of precursor was increased in the synthesis of Cu nanoparticles via the modified polyol process. When the reduction rate is high enough, the injection rate will be equal to the production rate. Hence, fast injection permits a short burst of nucleation, and generates many nuclei, because the concentration of metal atoms quickly reaches a critical supersaturation level, resulting in finer particles with a narrower size distribution.

The Sn nanoparticles shown in Fig. 1 are aggregated shapes consisting of several hundred-nanometer particles, instead of isolated ones. However, transmission electron microscopy (TEM) images of Sn nanoparticles synthesized via chemical reduction indicated a finer particle size of several tens of nanometers.^[9-14,16,17] Moreover, Hsiao *et al.*^[10] observed the particle size of Sn-3.0Ag-0.5Cu as a function of reaction time during reduction synthesis. They reported

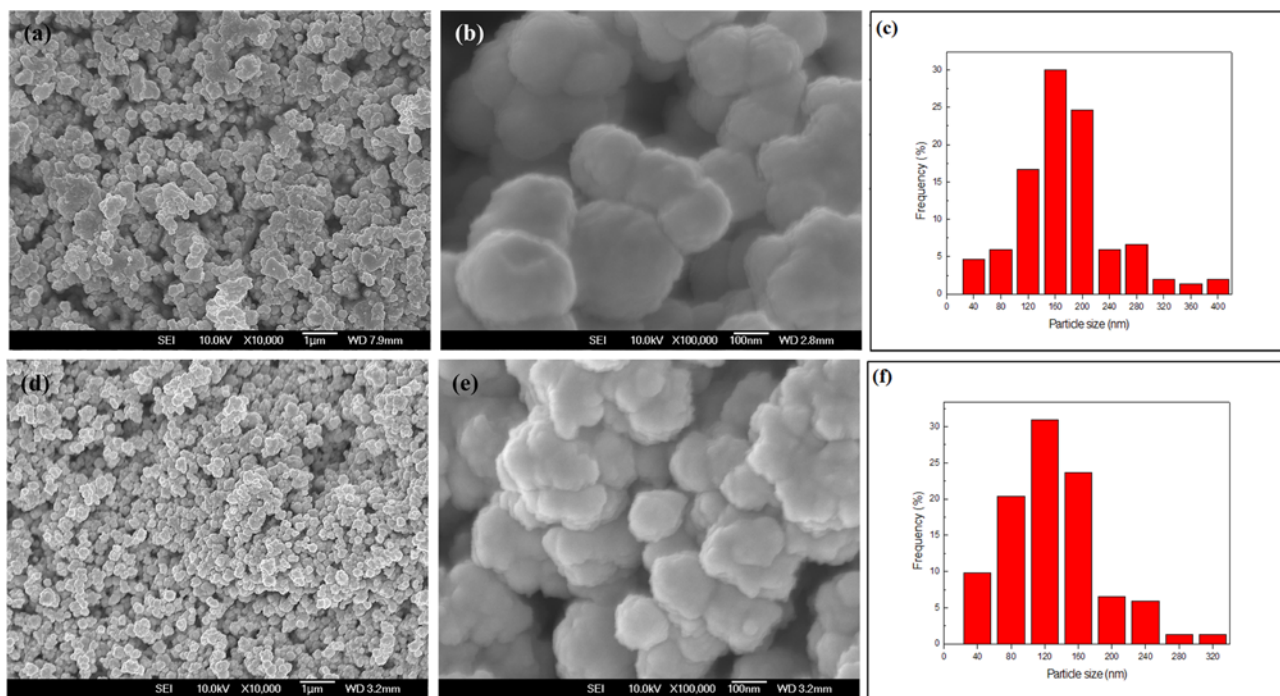


Fig. 1. SEM images and size distributions of Sn nanoparticles collected following different injection rates during synthesis in a methanol solution containing 1,10-phenanthroline monohydrate and sodium borohydride: (a, b, c) 1.5 ml/min and (d, e, f) 3 ml/min.

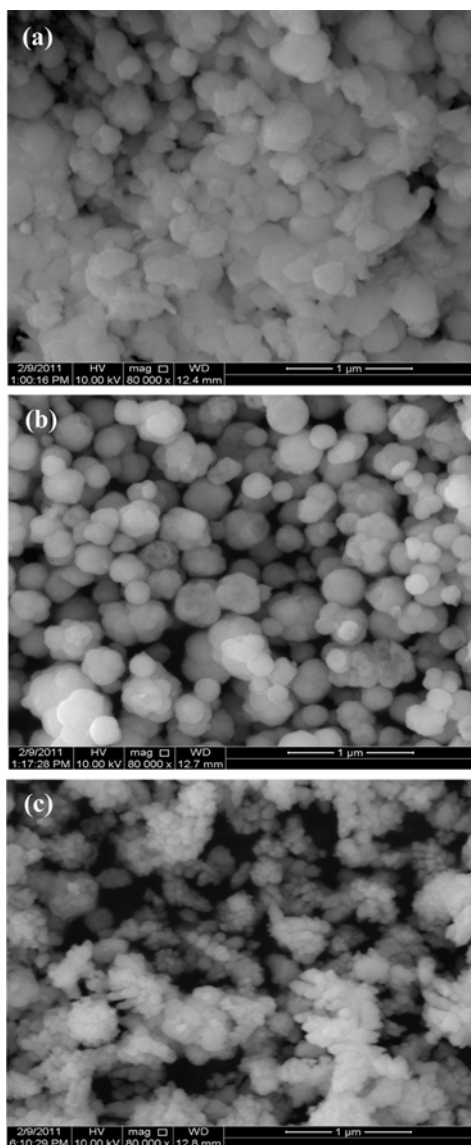


Fig. 2. SEM images of Sn nanoparticles dried at different temperatures after synthesis in a methanol solution containing 1,10-phenanthroline monohydrate: (a) 60 °C, (b) room temperature, and (c) freeze drying.

that Sn-3.0Ag-0.5Cu particles promptly grew up and saturated to several tens of nanometers after ~1 min, and named these the secondary particles, i.e., aggregates of as-precipitated primary particles. Hence, the particles in Fig. 1 are agglomerates of secondary particles, which are judged to be mainly attributable to the drying process.

The effect of temperature in the drying process can be deduced from Fig. 2, which shows SEM images of final samples dried at different temperatures. From Fig. 2, the agglomeration of particles can be seen to intensify as the drying temperature increases. The freeze-dried sample (Fig. 2(c)) shows aggregates consisting of particles of several tens of nanometers in diameter. Meanwhile, in Fig.

2(b), the sample dried at room temperature indicates very discrete particles of a few hundreds of nanometers, and particles of several tens of nanometers cannot be observed. Thus, it is concluded that the particles of a few hundreds of nanometers were formed by the agglomeration of several tens of nanometer sized particles, and we name these agglomerations tertiary particles. The sample dried at 60°C (Fig. 2(a)) represented aggregates of several hundred-nanometer particles, i.e., the initial stage of quaternary particles. Hence, the particles shown in Fig. 1 could be considered as aggregates of tertiary particles. Consequently, the degree of agglomeration of the resulting particles became severe as the drying temperature increased, resulting in an increase in the size of the final particles. Considering the surface characteristics of particles synthesized with the 1,10-phenanthroline monohydrate capping agent, it is expected that agglomeration to form tertiary particles is inevitable during drying, unless the solution is freeze dried. However, the room temperature drying process was an effective way of obstructing excessive agglomeration and formation of quaternary particles.

The influence of sonication can be identified from the distinctive morphology shown in Fig. 3. An injection rate of 3 ml/min was used to synthesize the particles in Fig. 3, and the reaction and drying temperatures were identical to the particles in Fig. 1. Turning on sonication during the holding step resulted in abnormal aggregates of nanoparticles, as well as slight agglomeration on the whole, forming large aggregates of several hundred micrometers consisting of nanoparticles of a few hundreds of nanometers. Thus, it is concluded that the sonication process preferentially brought about the coarsening of secondary particles to form tertiary particles, then induced aggregation of the tertiary particles. Considering the shape and size of the large aggregates, it is also estimated that the driving force of agglomeration by sonication is much higher than that by drying. Consequently, applying sonication accelerated both the agglomeration and aggregation considerably, even during the synthesis step.

The main mechanism of the aggregating behavior can be considered to be the collisions of nanoparticles activated into motion by sonication. The movement of nanoparticles synthesized in a normal condition would be regular due to the uni-directional stirring, and thus the particle collisions occurred not only at low frequency but also with low energy, mainly failing to form aggregates. In contrast, particles activated with the aid of sonication could exhibit vigorous and irregular individual movements. Hence, particle collisions could occur with a higher energy and frequency, resulting in the formation of aggregates. Under the same sonication energy, it is likely that the movement of small particles is more vigorous than that of large particles. Therefore, secondary particles could coarsen easily during

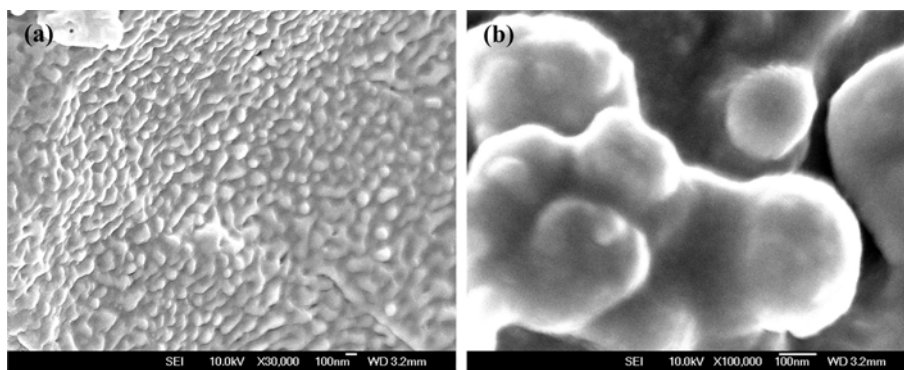


Fig. 3. SEM images of Sn nanoparticles collected after a holding step of 1 h in an ultrasonic bath following injection during synthesis in a methanol solution containing 1,10-phenanthroline monohydrate: (a) lower and (b) higher magnification.

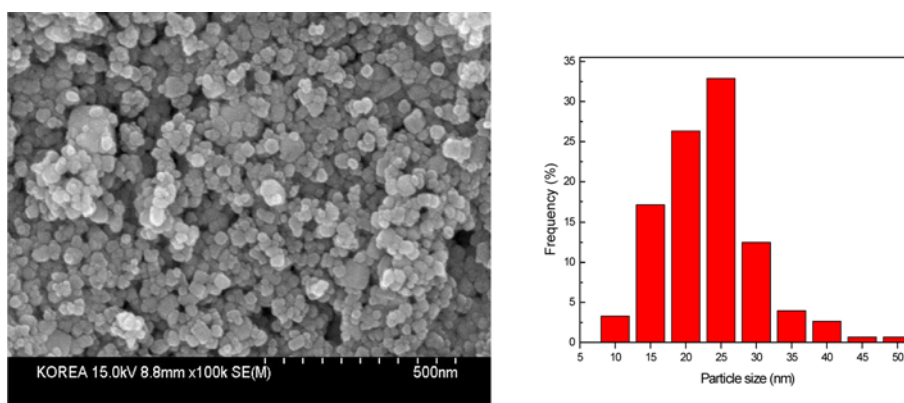


Fig. 4. SEM image and size distribution of Sn nanoparticles synthesized at room temperature in a DEG solution containing PVP.

sonication, while the tertiary particles just aggregated with one another.

As the capping agent, 1,10-phenanthroline monohydrate, was observed to be relatively ineffective in preventing agglomeration and aggregation between particles during and after synthesis, another nanoparticle synthesis experiment was performed in a solution containing PVP, which is a well-known capping agent for nanoparticles. Figure 4 shows SEM images of the final Sn nanoparticles collected when the reaction medium and capping agent were exchanged with DEG and PVP, respectively. The injection rate of tin(II) 2-ethylhexanoate precursor was 3 ml/min, which is identical to the particles in Fig. 1(d, e), and the reaction and drying temperature were also the same as for those in Fig. 1. The size of the Sn nanoparticles collected was measured as 8-85 nm in diameter (average diameter = 26.0 nm). Thus, the final size of nanoparticles decreased significantly by applying the DEG medium containing PVP, implying that PVP is more effective than 1,10-phenanthroline monohydrate in suppressing the agglomeration into tertiary level particles during drying. Nevertheless, it was observed that aggregation after drying was still problematic. The sticky surface characteristics of Sn nano-

particles encapsulated with PVP may induce aggregation between the nanoparticles during drying. In summary, the combination of PVP and DEG is more effective than that of 1,10-phenanthroline monohydrate and methanol in preventing agglomeration between nanoparticles during drying. However, further research into a complete process to avoid aggregation between particles during drying is required.

As the 1,10-phenanthroline monohydrate is an organic compound, which forms strong complexes with most metal ions, it would be insufficient to form the thick capping layers that interrupt the agglomeration between nanoparticles. In contrast, PVP is a polymer material that can thickly encapsulate the synthesized Sn nanoparticles, thus disturbing the agglomeration behavior more effectively and stably.

Images of the final Sn nanoparticles, when the reaction temperature was increased to 40°C and 80°C in the solution containing PVP, are shown in Fig. 5. With a reaction temperature of 40°C, the final size of the Sn nanoparticles was found to be 15-80 nm in diameter (average diameter = 33.0 nm) (Fig. 5(a)), which is slightly larger than the particles in Fig. 4. At a temperature of 80°C, as shown in Fig.

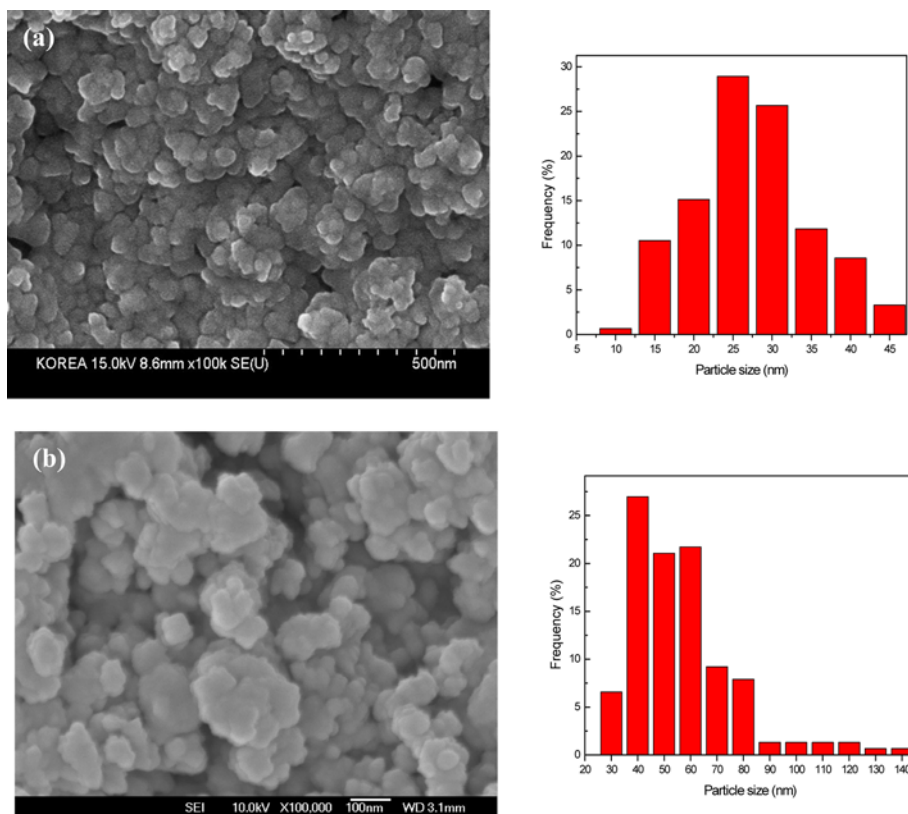


Fig. 5. SEM images and size distributions of Sn nanoparticles synthesized at different reaction temperatures in a DEG solution containing PVP: (a) 40°C and (c) 80°C.

5(b), however, the size of Sn nanoparticles was 20–136 nm (average diameter = 53.9 nm), and thus a conspicuous increase was found in particle size. Therefore, the resultant particle size becomes larger as the reaction temperature increases. By analyzing the size distribution results, the increase in average size was attributed to the pronounced increase in the size of the largest particles. The bigger particles synthesized at 80°C were likely to have been formed by the agglomeration of secondary particles, a result of more vigorous particle movement due to the thermal energy available during the synthesis reaction. Considering the identical drying conditions, it is apparent that the reaction temperature during the synthesis directly affects the size of the resultant particles.^[17,18] Consequently, the reduction temperature, as well as the injection rate, was fairly effective in controlling the size of Sn nanoparticles.

4. CONCLUSIONS

By observing the changes in the size and morphology of Sn nanoparticles synthesized via chemical reduction with respect to the injection rate of a precursor solution, application of sonication, types of reaction medium and capping agent, reaction temperature, and drying temperature, the

following results were observed. In methanol solutions containing 1,10-phenanthroline monohydrate, the size of Sn nanoparticles collected after synthesis decreased as the injection rate increased. In addition, higher drying temperatures accelerated agglomeration between Sn nanoparticles. The application of sonication accelerated agglomerating and aggregating behaviors between nanoparticles, which was detrimental to the collection of separated nanoparticles. In comparison to the synthesis in methanol solution containing 1,10-phenanthroline monohydrate, the Sn nanoparticles synthesized in DEG solution containing PVP exhibited an outstandingly small size, mainly due to the suppression of agglomeration during drying. In this case, the resultant particle size increased with higher reaction temperatures.

ACKNOWLEDGMENTS

This work was financially supported by the Korea Institute of Energy Technology Evaluation and Planning (KETEP) (20102020100300).

REFERENCES

1. Y. M. Kim, K.-M. Harr, and Y.-H. Kim, *Electron. Mater.*

- Lett.* **6**, 151 (2010).
2. W. Ki, Y.-K. Lee, C.-W. Lee, and S. Yoo, *J. Microelectron. Packag. Soc.* **18**, 9 (2011).
 3. A.-M. Yu, M.-S. Kim, C.-W. Lee, and J.-H. Lee, *Met. Mater. Int.* **17**, 521 (2011).
 4. E. H. Amalu, W. K. Lau, N. N. Ekere, R. S. Bhatti, S. Mallik, K. C. Otiaba, and G. Takyi, *Microelectron. Eng.* **88**, 1610 (2011).
 5. T.-N. Tsai, *Robot. Comput. Integrated Manuf.* **27**, 808 (2011).
 6. C. D. Zou, Y. L. Gao, B. Yang, X. Z. Xia, Q. J. Zhai, C. Andersson, and J. Liu, *J. Electron. Mater.* **38**, 351 (2009).
 7. Y. Gao, C. Zou, B. Yang, Q. Zhai, J. Liu, E. Zhuravlev, and C. Schick, *J. Alloys Compd.* **484**, 777 (2009).
 8. C. D. Zou, Y. L. Gao, B. Yang, Q. J. Zhai, C. Andersson, and J. Liu, *Solder. Surf. Mount Technol.* **21**, 9 (2009).
 9. H. Jiang, K. Moon, H. Dong, F. Hua, and C. P. Wong, *Chem. Phys. Lett.* **429**, 492 (2006).
 10. L.-Y. Hsiao and J.-G. Duh, *J. Electron. Mater.* **35**, 1755 (2006).
 11. H. Jiang, K. Moon, F. Hua, and C. P. Wong, *Chem. Mater.* **19**, 4482 (2007).
 12. P.-C. Huang and J.-G. Duh, *Proc. 58th ECTC*, p. 431, IEEE CPMT, Orlando, US (2008).
 13. H. Jiang, K. Moon, and C. P. Wong, *Proc. 58th ECTC*, p. 1400, IEEE CPMT, Orlando, US (2008).
 14. C. Y. Lin, U. S. Mohanty, and J. H. Chou, *J. Alloys Compd.* **472**, 281 (2009).
 15. C. Zou, Y. Gao, B. Yang, and Q. Zhai, *J. Mater. Sci.: Mater. Electron.* **21**, 868 (2010).
 16. C. Y. Lin, U. S. Mohanty, and J. H. Chou, *J. Alloys Compd.* **501**, 204 (2010).
 17. Y. H. Jo, J. C. Park, J. U. Band, H. Song, and H. M. Lee, *J. Nanosci. Nanotechnol.* **11**, 1037 (2011).
 18. B. K. Park, S. Jeong, D. Kim, J. Moon, S. Lim, and J. S. Kim, *J. Colloid Interface Sci.* **311**, 417 (2007).